INSTITUTE OF PHYSICS PUBLISHING JOURNAL OF OPTICS A: PURE AND APPLIED OPTICS

J. Opt. A: Pure Appl. Opt. **8** (2006) 259–267 doi:10.1088/1464-4258/8/3/006

Study of resonant modes of a periodic metallic array near a dielectric interface: evanescent-to-propagating coupling via surface plasmon excitation

Diana C Skigin[1,3] **and Marcelo Lester**[2,3]

[1] Grupo de Electromagnetismo Aplicado, Departamento de Física, Facultad de Ciencias Exactas y Naturales, Universidad de Buenos Aires, Ciudad Universitaria, Pabellón I, C1428EHA Buenos Aires, Argentina

[2] Instituto de Física Arroyo Seco, Facultad de Ciencias Exactas, Universidad Nacional del Centro de la Provincia de Buenos Aires, Pinto 399 (cp 7000) Buenos Aires, Argentina

Received 11 October 2005, accepted for publication 10 January 2006
Published 7 February 2006
Online at stacks.iop.org/JOptA/8/259

Abstract

The structural modes of a 2D periodic array of metallic cylinders near a dielectric interface are studied, for large and small wavelength-to-period ratios. We show that there are two clearly distinguished kinds of resonances: waveguide modes of the gap between the array and the interface, and eigenmode excitations (plasmons). While waveguide modes are present for both polarizations, surface plasmon polaritons (SPPs) only occur for p polarization, and, under particular conditions, this mechanism can produce an efficient coupling (about 60%) between the incident evanescent wave and the eigenmodes supported by the structure, which produces an enhanced transmitted propagating order. The response of the structure is analysed in detail by varying its relevant parameters, paying particular attention to the interplay between SPPs and Rayleigh anomalies, and its effect on the grating response.

Keywords: grating–waveguide structures, resonances, anomaly, surface plasmons, enhanced transmission

1. Introduction

In recent years great effort has been devoted to understanding the physical mechanism involved in extraordinary (enhanced) optical transmission through periodic systems made up by subwavelength slits [1–4] or two-dimensional holes in a metallic plate [5–7].

Two main mechanisms have been proposed as responsible for the field enhancement:

(i) excitation of surface waves or eigenmodes of the structure in 1D and 2D structures, and
(ii) structural resonances in subwavelength slits or arrays of narrow slits (Fabry–Perot-like behaviour) in 1D periodic systems.

[3] Consejo Nacional de Investigaciones Científicas y Técnicas CONICET.

Surface waves are electromagnetic fields that propagate parallel to the interface and whose amplitudes are exponentially decaying in the normal direction [8, 9]. These eigenmodes can be found in metal–dielectric interfaces, in which case they are identified as surface plasmons [10–13], as well as in dielectric–dielectric interfaces [14, 15].

On the other hand, structural resonances in narrow slits are originated by constructive interference of multiple reflections into each nano- or micro-cavity, and a periodic array of narrow slits (grating) acts as an amplifier of these individual resonances [1–3, 8].

Besides, in periodic structures such as diffraction gratings or arrays of cylinders or holes, another mechanism takes place, which is founded in the pseudo-periodic nature of the diffracted field. This physical mechanism is responsible for propagating

as well as for surface (grazing) modes, known as Rayleigh anomalies [16, 17].

The resonant coupling between the incident radiation and the different eigenmodes supported by the structure gives rise to a large variety of electromagnetic effects, such as enhanced transmission [5, 6, 18–20], suppression of transmission [21], forbidden bands [1, 22, 23], near field intensification [24–26], etc, depending on the relationship between the incident wavelength and the geometrical and constitutive parameters of the structure. Some of these phenomena already have concrete technological applications in near-field microscopy [25], imaging [27, 28], medical diagnostics [29, 30], optical communications and computing [31], and many other potential applications that are being investigated.

Several studies have considered a diffraction grating on a single- or multiple-layer substrate as a system to get a particular electromagnetic response. The capability of such systems to couple the incident radiation to the eigenmodes of the structure makes them attractive for different purposes. In particular, the incoming radiation can be coupled and re-directed to particular directions [32, 33], it can be used to guide a mode in a planar waveguide [31], or it can produce sharp variations in the reflected/transmitted response [34, 35]. The interplay between the excitation of different kinds of eigenmodes, provides a rich variety of effects.

In this paper we investigate in detail the behaviour of a periodic array of metallic nanowires, when illuminated by a propagating or an evanescent wave. We analyse the transmitted and reflected response of the system, and study the different kinds of resonances that occur in this structure for a wide range of wavelengths, and for both polarization modes. In particular, SPP modes can be used to efficiently couple an evanescent wave to a propagating diffraction order. Also, the dynamics of the structure is analysed in view of the waveguide and SPP modes, and the Rayleigh anomalies. In section 2 we summarize the modal approach used to calculate the response of the structure, and in section 3 we discuss the results obtained. We show maps of reflected and transmitted efficiency, varying the period of the array and the distance to the interface. Finally, some conclusions are summarized in section 4.

2. Modal approach

We consider a 2D periodic array of metallic wires near a dielectric interface (see figure 1). The interface is at $y = 0$ and the half-space $y < 0$ is filled by a non-magnetic material ($\mu_1 = 1$) with a permittivity ε_1. The periodic array is immersed in air ($\varepsilon_0 = 1, \mu_0 = 1$), and is at a distance e from the interface. The period of the structure is d, the wires have a square cross section of side h and a complex dielectric constant ε_2. The system is illuminated from $y < 0$ by a plane wave, forming an angle θ_1 with the y axis. The incident wavevector is $\vec{k}_1 = k_1(\sin\theta_1\hat{x} + \cos\theta_1\hat{y})$, with $k_1 = \sqrt{\varepsilon_1}k_0$, $k_0 = 2\pi/\lambda_0$, λ_0 being the wavelength in vacuum. The incidence plane is parallel to the (x, y) plane, and both fundamental modes of polarization are considered: s (electric field perpendicular to the incidence plane) and p (electric field parallel to the incidence plane). The diffraction problem is solved using the modal method for highly conducting wire gratings [36], extended to consider

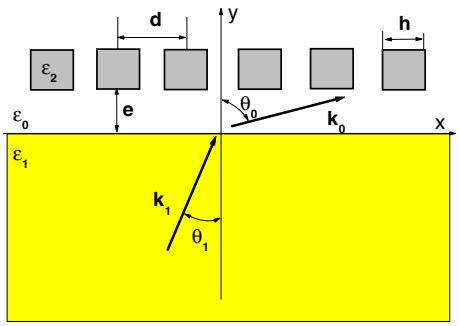

Figure 1. Geometry of the system.
(This figure is in colour only in the electronic version)

additional dielectric interfaces. We denote f^{s} (f^{p}) to the electric (magnetic) field in the s (p) polarization case. The space is divided into regions, separated by horizontal interfaces at $y = 0$, $y = e$, and $y = e+h$. The reflected field in $y \leqslant 0$ and the transmitted field in $y \geqslant e + h$ are represented by outgoing Rayleigh expansions. Then, the field in these regions is given by

$$f^q_{y\leqslant 0}(x, y) = \exp[\mathrm{i}(\alpha_1 x + \beta^1_1 y)] + \sum_n R^q_n \exp[\mathrm{i}(\alpha_n x - \beta^1_n y)], \tag{1}$$

and

$$f^q_{y\geqslant e+h}(x, y) = \sum_n T^q_n \exp[\mathrm{i}(\alpha_n x + \beta^0_n (y - (e + h)))], \tag{2}$$

respectively, here $\alpha_n = (2\pi/\lambda_0)\sin\theta_0 + n(2\pi/d)$, $(\beta^j_n)^2 = (2\pi/\lambda_0)^2\varepsilon_j - \alpha^2_n$, θ_0 is the angle of incidence in the air region (see figure 1), the superscript j denotes the region, and R^q_n and T^q_n are the reflected and transmitted Rayleigh amplitudes, respectively ($q = \mathrm{s}, \mathrm{p}$ denotes the polarization mode). In the layer between the interface and the array ($0 \leqslant y \leqslant e$), the field is represented by a combination of up and down plane waves,

$$f^q_{0\leqslant y\leqslant e}(x, y) = \sum_n A^q_n \exp[\mathrm{i}(\alpha_n x - \beta^0_n y)] + \sum_n B^q_n \exp[\mathrm{i}(\alpha_n x + \beta^0_n y)], \tag{3}$$

and inside the slits ($e \leqslant y \leqslant e + h$) the fields are expanded in terms of eigenfunctions that take into account the SIBC on the lateral walls of each slit [36]:

$$f^q_{e\leqslant y\leqslant e+h}(x, y) = \sum_{m=0}^{\infty} U^q_m(x) w^q_m(y), \tag{4}$$

where

$$U^{\mathrm{s}}_m(x) = \sin(u^{\mathrm{s}}_m x) + \eta^{\mathrm{s}} u^{\mathrm{s}}_m \cos(u^{\mathrm{s}}_m x), \tag{5}$$

$$U^{\mathrm{p}}_m(x) = \frac{\eta^{\mathrm{p}}}{u^{\mathrm{p}}_m}\sin(u^{\mathrm{p}}_m x) + \cos(u^{\mathrm{p}}_m x), \tag{6}$$

$$w^q_m(y) = a^q_m \cos(v_m y) + b^q_m \sin(v_m y), \qquad q = \mathrm{s}, \mathrm{p} \tag{7}$$

$$(v^q_m)^2 = k^2_0 - (u^q_m)^2, \qquad q = \mathrm{s}, \mathrm{p} \tag{8}$$

$$\eta^{\mathrm{s}} = \frac{\mathrm{i}\mathcal{Z}}{k_0} = \frac{\mathrm{i}}{\sqrt{\varepsilon_2}k_0}, \tag{9}$$

$$\eta^{\mathrm{p}} = \frac{k_0 \mathcal{Z}}{\mathrm{i}} = \frac{k_0}{\sqrt{\varepsilon_2}\mathrm{i}}, \tag{10}$$

and a_m^q and b_m^q are unknown complex amplitudes. The quantities u_m^{s} and u_m^{p} are determined by the following eigenvalues equations, that come from imposing the SIBC on the vertical walls of the slits:

$$\begin{aligned} \tan(u_m^{\mathrm{s}} c) &= \frac{2\eta^{\mathrm{s}} u_m^{\mathrm{s}}}{(\eta^{\mathrm{s}} u_m^{\mathrm{s}})^2 - 1} \qquad \text{for s polarization} \\ \tan(u_m^{\mathrm{p}} c) &= \frac{2\eta^{\mathrm{p}} u_m^{\mathrm{p}}}{(u_m^{\mathrm{p}})^2 - (\eta^{\mathrm{p}})^2} \qquad \text{for p polarization,} \end{aligned} \tag{11}$$

where $c = d - h$ is the slit width. The fields are matched at the horizontal interfaces by imposing the continuity of the tangential components in the open sections, and by applying the SIBC in the metallic regions. The x-dependent equation that arises from the continuity of the tangential electric field over the whole period is projected onto the basis $\{\exp(\mathrm{i}\alpha_n x)\}$, whereas the equation that results from the continuity of the tangential magnetic field, which is only valid in the region between wires, is projected onto the set $\{U_m^q(x)\}$, which forms a complete and orthogonal basis in this interval. This method leads to a system of coupled equations that can be put in matrix form, which has to be solved for the unknown reflected and transmitted amplitudes.

The results obtained have been checked for convergence and the energy balance is satisfied within an error of 1% in all the examples shown below. Among the comparisons with published results used to validate the method, we reproduced the transmission results of a nanowire-grid polarizer (table 1 of [37]) within an error of 1%.

3. Results

The periodic structure can be illuminated by two different kinds of waves: propagating waves, for incidence angles $\theta_1 < \theta_{\mathrm{c}}$, with $\theta_{\mathrm{c}} = \arcsin\sqrt{\varepsilon_0/\varepsilon_1}$, and evanescent waves generated by total internal reflection, which decay in the direction $y \geqslant 0$, for incidence angles $\theta_1 \geqslant \theta_{\mathrm{c}}$ [38, 39]. In this section we analyse the response of the array in both incidence cases, and study the evolution of the effects caused by the different structural resonances in the transmitted and reflected responses of the structure, when the period and the array–interface distance (e) is varied.

3.1. Waveguide resonances

We start by considering periodic arrays that can only support a single transmitted and reflected (specular) orders. For large values of λ_0/d, the cylinder array is expected to behave like a metallic thin film. Therefore, a waveguide is formed between the dielectric interface and the array, and the whole structure can be regarded as a four-region planar multilayer system with a dielectric substrate (ε_1), a waveguide (ε_0), a metallic thin film (ε_2), and the vacuum superstrate [32, 40, 41]. If the thickness of the equivalent metallic layer—which is related to the typical size of the cylinders—is large, no transmitted field is expected since the electromagnetic field is absorbed in the metal. However, if the metallic layer is thin enough, a transmitted field can be obtained for certain incidence conditions, depending on the vacuum waveguide thickness.

In figure 2 we show maps of total reflected and transmitted intensity as a function of the effective waveguide thickness e^*/λ_0 and of the incidence angle. The effective thickness is defined as $e^* = e + \Delta$, where e is the array-to-interface distance and Δ is a correction introduced for each one of the polarization modes. Figures 2(a) and (b) are the maps for s polarization and figures 2(c) and (d) correspond to p polarization. The incident wavelength is $\lambda_0 = 650$ nm, and the period of the array is set to $d = 162.5$ nm, such that $\lambda_0/d = 4$. The cylinders are made of silver ($\varepsilon_2 = -17.02 + \mathrm{i}1.15$), have a square cross section of side $h = 111$ nm, and are immersed in air; the dielectric constant of the incident medium is $\varepsilon_1 = 3.24$, which implies that $\theta_{\mathrm{c}} = 33.75°$. The reflected intensity is calculated inside the dielectric substrate.

The maps for s and p polarizations have some common features. For incidence angles greater than θ_{c}, total internal reflection occurs at the dielectric interface, and then most of the field is reflected by the structure and no transmitted field is found. For small enough values of the distance e, part of the field is absorbed by the metallic array, which reduces the reflected field, as observed in figures 2(a) and (c) for $\theta \sim \theta_{\mathrm{c}}$. For $\theta \leqslant \theta_{\mathrm{c}}$, several regularly spaced minima appear in the reflected intensity maps. These minima correspond to structural resonances, and are characterized by a strongly localized electromagnetic field between the array and the interface. These resonances are produced by multiple reflections between the periodic structure and the interface (see [39]). In this case, the periodic array works like a homogeneous metal ($\lambda_0/d = 4$) and the periodicity is only a perturbative correction.

If the skin effect is neglected, the structural resonances would occur for

$$\cos(\theta_0^{\mathrm{res}}) = n\frac{\lambda_0}{2e}; \qquad \text{for } n = 0, 1, 2, \ldots. \tag{12}$$

In terms of the incidence angle θ_1, and using Snell's law,

$$\sin(\theta_1^{\mathrm{res}}) = \frac{1}{\sqrt{\varepsilon_1}}\sin(\theta_0^{\mathrm{res}}). \tag{13}$$

When $0.5 < e/\lambda_0 < 1$, there is only one angle of incidence for which equation (12) is satisfied ($n = 1$). This is observed in the reflected intensity maps, since in this interval only one minimum is found for a fixed value of e/λ_0. In analogy with hollow waveguides, we can say that the system supports only 'one channel'. However, if $1 < e/\lambda_0 < 1.5$, a new channel can be supported, which corresponds to $n = 2$. As e/λ_0 increases further, new waveguide modes are opened up each time the relationship $n/2 < e/\lambda_0 < (n+1)/2$ is fulfilled, for integer n. These resonances produce the behaviour observed in the plots: for a given value of e, the reflectivity has a fixed number of minima for different incidence angles θ_1^{res}, whose width decreases as the angle approaches θ_{c}. These resonances are purely structural, and are not connected with the metallic characteristic of the cylinders but only with the geometrical parameters e/λ_0 and λ_0/d.

In figure 2 the curves obtained from equation (12) are superimposed on the reflectivity maps. An excellent agreement between these curves and the dark fringes (low

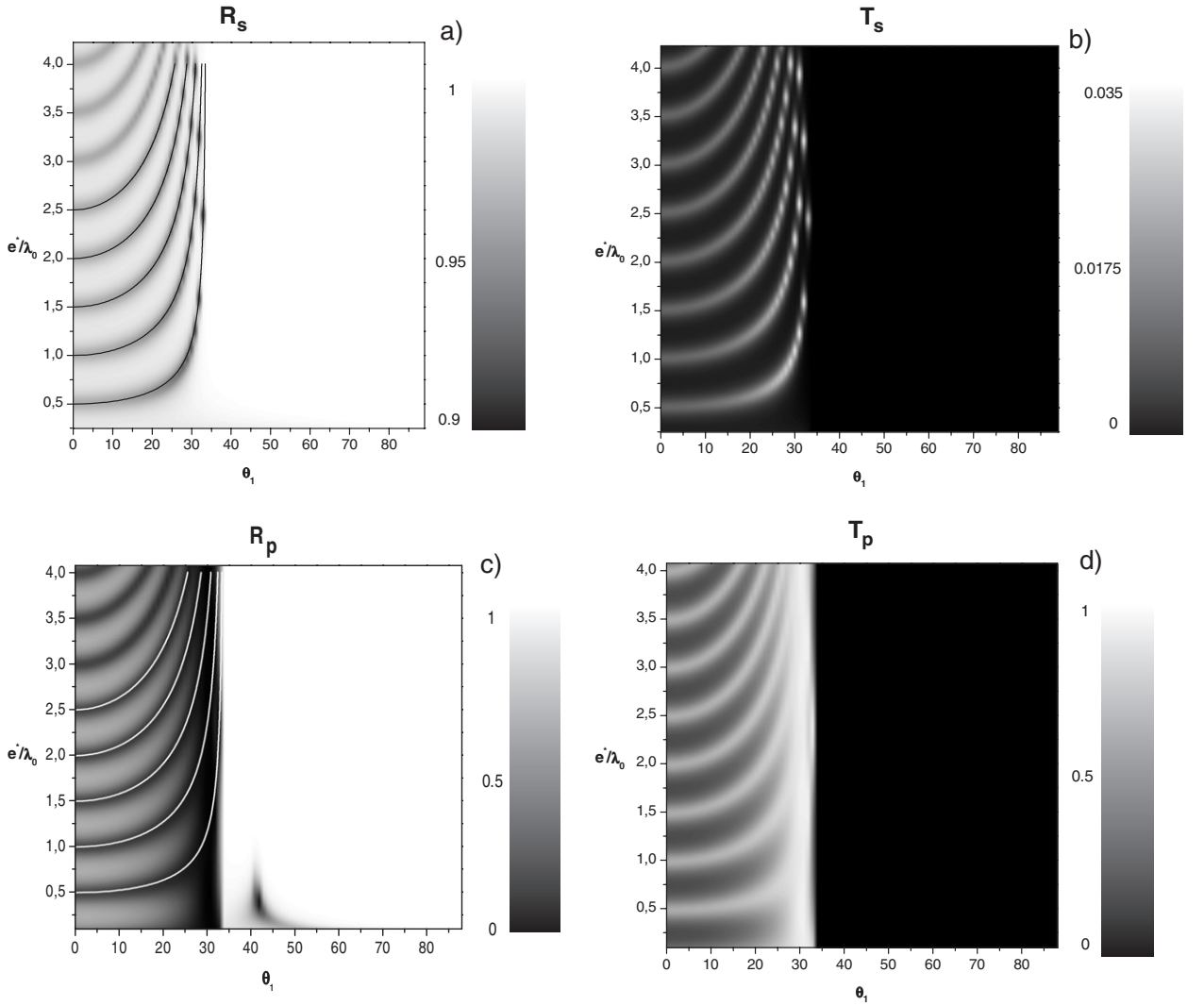

Figure 2. Maps of total reflected and transmitted intensity as a function of e^*/λ_0 and θ_1, for $\lambda_0 = 650$ nm, $d = 162.5$ nm, $h = 111$ nm, $\varepsilon_0 = 1$, $\varepsilon_1 = 3.24$, $\varepsilon_2 = -17.02 + \mathrm{i}1.15$. (a) Reflected intensity and s polarization; (b) transmitted intensity and s polarization; (c) reflected intensity and p polarization; (d) transmitted intensity and p polarization.

reflectivity) occurs when instead of e we introduce the effective thickness $e^* = e + \Delta$ in equation (12). Due to the finite conductivity of the cylinders, the electromagnetic field penetrates into the metallic structure (skin effect) [38, 42, 43], and this produces an effective waveguide—formed between the dielectric interface and the array—with a larger width. Then, the resonant thicknesses are also modified [2, 21]. Therefore, the agreement between equation (12) and the response of the structure is better met for e^*. Even though this structural effect is present in both polarizations, there is an additional reflectivity minimum for $25° < \theta_1 < \theta_c$, only for the p case (figure 2(c)). This minimum appears as a dark vertical fringe in the contour plot, and corresponds to the Brewster angle of the dielectric–air interface. Once again, the presence of the metallic array does not appear to affect the response of the structure for this value of λ_0/d.

Another distinct characteristic of the p map (figure 2(c)) is the behaviour of the reflectivity for small values of e/λ_0, i.e., when the array is very close to the interface. In this case, the reflectivity decreases significantly for $\theta \gtrsim \theta_c$. When the angle of incidence exceeds the critical angle, it is possible to excite an eigenmode of the periodic metallic structure when the electromagnetic wave is p polarized, and this produces a significant power absorption. For the set of geometrical parameters used in this map, it is not possible to excite these eigenmodes (surface plasmon polaritons) by a propagating incident wave, and then, the resonance is obtained for $\theta > \theta_c$, i.e., when the wave incident on the array is evanescent. In the following section we analyse and discuss the SPPs and their effects on the structure response for different wavelength-to-period ratios.

3.2. Surface plasmon excitations

If the array is regarded as a metallic surface, in first approximation the momentum associated with the surface plasmon is given by

$$\kappa = k_0 \sqrt{\frac{\varepsilon_2}{\varepsilon_2 + \varepsilon_0}}, \tag{14}$$

or

$$\hat{\kappa} = \frac{\kappa}{k_0} = \sqrt{\frac{\varepsilon_r}{\varepsilon_r + 1}}, \qquad \varepsilon_r = \varepsilon_2/\varepsilon_0. \tag{15}$$

$\hat{\kappa}$ is in general a complex quantity, and the double sign of the square root represents surface modes propagating in opposite directions. Since $|\mathrm{Re}[\hat{\kappa}]| > 1$, these modes can couple to an inhomogeneous wave if the coupling condition $\hat{k}_{0x} = \alpha_0/k_0 = \mathrm{Re}[\hat{\kappa}]$, is satisfied. Analogously to what occurs in the excitation of a surface plasmon by TIR in a prism [12, 26, 40], the efficiency of the coupling is mainly governed by the distance between the periodic structure and the interface, and, in a second order, by the cylinders' cross section [44].

If the ratio λ_0/d is small enough, it is possible to have diffractive effects due to the contribution of extra momentum provided by the periodic array $\vec{K} = (2\pi/d)\,\hat{x}$. Then, the family of diffracted plasmons propagating in the $\hat{x}$ direction is given by

$$\kappa_n = \kappa + nK. \tag{16}$$

Dividing equation (16) by k_0 and defining $\hat{\kappa}_n = \kappa_n/k_0$ we get

$$\hat{\kappa}_n = \hat{\kappa} + n\frac{\lambda_0}{d}. \tag{17}$$

If we identify $\mathrm{Re}[\hat{\kappa}_n]$ with $\sin\theta_{0n}$ in such a way that $(\beta_n^0)^2$ takes a real value, the surface plasmon can be diffracted and coupled to a propagating wave. Then, the eigenmode excited by the evanescent wave is diffracted by the periodic array in certain particular directions. A similar reasoning can be applied to the incident evanescent wave. The evanescent wave is diffracted by the periodic array when the grating equation is satisfied [16]:

$$\sin\theta_{0n} = \sqrt{\varepsilon_1}\sin\theta_1 + n\frac{\lambda_0}{d}, \tag{18}$$

and these orders are propagating orders if $(\cos\theta_{0n})^2 = \varepsilon_0 - (\sin\theta_{0n})^2 < 1$, regardless of the incident wave polarization. For the p mode, if the momentum associated with the evanescent wave in the $\hat{x}$ direction ($\sqrt{\varepsilon_1}\sin\theta_1$) is close to $\hat{\kappa}$ (SPP excitation), the incident wave is diffracted and gives rise to propagating orders in the same directions corresponding to the surface plasmon diffraction. Then, for the p mode it is possible to get an enhancement of the transmitted orders via the surface plasmon excitation.

In figure 3 we show maps of the total reflected and transmitted efficiency, as a function of the incidence angle and of the array period d for an array located at a distance $e = 0.25\lambda_0 = 179.25$ nm, for s (figures 3(a) and (b)) and p (figures 3(c) and (d)) polarizations. The side of the square cross section of the cylinders is $h = 456.2$ nm, the incident wavelength is $\lambda_0 = 717$ nm (at which the permittivity of silver is $\varepsilon_2 = -21.6 + \mathrm{i}1.36$), and $\varepsilon_1 = 2.25$. For these parameters, the critical angle is $\theta_c = 41.8°$, and consequently, different behaviours of the structure response are found for both polarizations, for $\theta_1 > \theta_c$ and for $\theta_1 < \theta_c$. In this case no structural resonances are expected, due to a smaller ratio λ_0/d.

For $d < 814$ nm a high reflectivity is found in the s case, for all incidence angles. For $\theta_1 > \theta_c$, total internal reflection in the dielectric–air interface governs the response of the structure. However, for $\theta_1 < \theta_c$ the reason for a high reflectivity is different. Since the size of the cylinders is fixed, as the period increases the width of the slits between cylinders also increases. Then, for $d = 814$ nm, the slit width is 358 nm, which roughly corresponds to $\lambda_0/2$. Consequently, for slit widths smaller than $\lambda_0/2$ no transmission is expected, whereas for slit widths larger than $\lambda_0/2$ some transmission is found, what modifies also the reflected response. For $\theta_1 > \approx \theta_c$ there is also some transmission, especially for $d > 814$ nm. This transmission is the result of the coupling of the evanescent wave generated at the planar interface with the array, by tunnel effect. It reaches up to the 20% of the total incoming power, when $d \approx 1.7\lambda_0 = 1218.9$ nm, at most (see figure 3(b)).

The array transforms the decaying wave in a propagating wave, and diffracts it in the forward direction. This effect is independent of the material of the cylinders, and could even be found if the metallic array were replaced by a dielectric one [32]. The fundamental condition for this kind of coupling is the proximity between the systems, in this case, the interface and the array. The response of the same system under p-polarized illumination, on the other hand, has other interesting features. Even though there is a clear definition of the critical angle (vertical line for $\theta_0 = 41.8°$), a significant amount of power is obtained on both sides, i.e., either for propagating or for evanescent waves incident on the metallic array (figures 3(c) and (d)). For a propagating incident wave, the incoming power is divided into reflected and transmitted in similar amounts. It is important to remark that this is not a general feature but a characteristic of the set of parameters chosen for this example. For $d = 814$ nm, a horizontal line can be appreciated in the p maps (figures 3(c) and (d)). As stated above, the slit width for this value of d is approximately $\lambda_0/2$, and then a new mode becomes propagating within the slit, which produces an anomaly in the reflected/transmitted response. The resonant period depends not only on the slit width but also on the permittivity of the metal [2, 21].

For $\theta_1 > \theta_c$, and especially for 473 nm $\leqslant d \leqslant$ 840 nm, there is a wide region in which the reflectivity is low, and a high transmission rate is found (figure 3(d)). This increase in the transmission for an incident evanescent wave is the result of the coupling between the incoming wave and the SPP supported by the structure, as explained above. The proximity of the array to the interface is exploited not only to convert an evanescent into a propagating wave, but also to couple this wave to an eigenmode of the metallic array, thus producing an enhancement of the transmitted intensity, which in this example reaches a maximum of 60% of the total incoming power (for $d = 817$ nm and $\theta_1 = 46°$). The evanescent eigenmode or surface plasmon can be transformed into a propagating wave and it is possible to transmit light for angles greater than the critical one. For these parameters, only the -1 and -2 transmitted orders are propagating, and the total transmitted intensity is distributed between both in similar amounts (not shown). In this case, the p-transmitted orders carry up to five orders of magnitude more power than their s polarization counterparts, for the same situation.

In figure 4 we show plots of the response of the system when the periodic structure is located further from the dielectric interface ($e/\lambda_0 = 0.75$). In this case, the transmission effects for $\theta > \theta_c$ weaken considerably for both

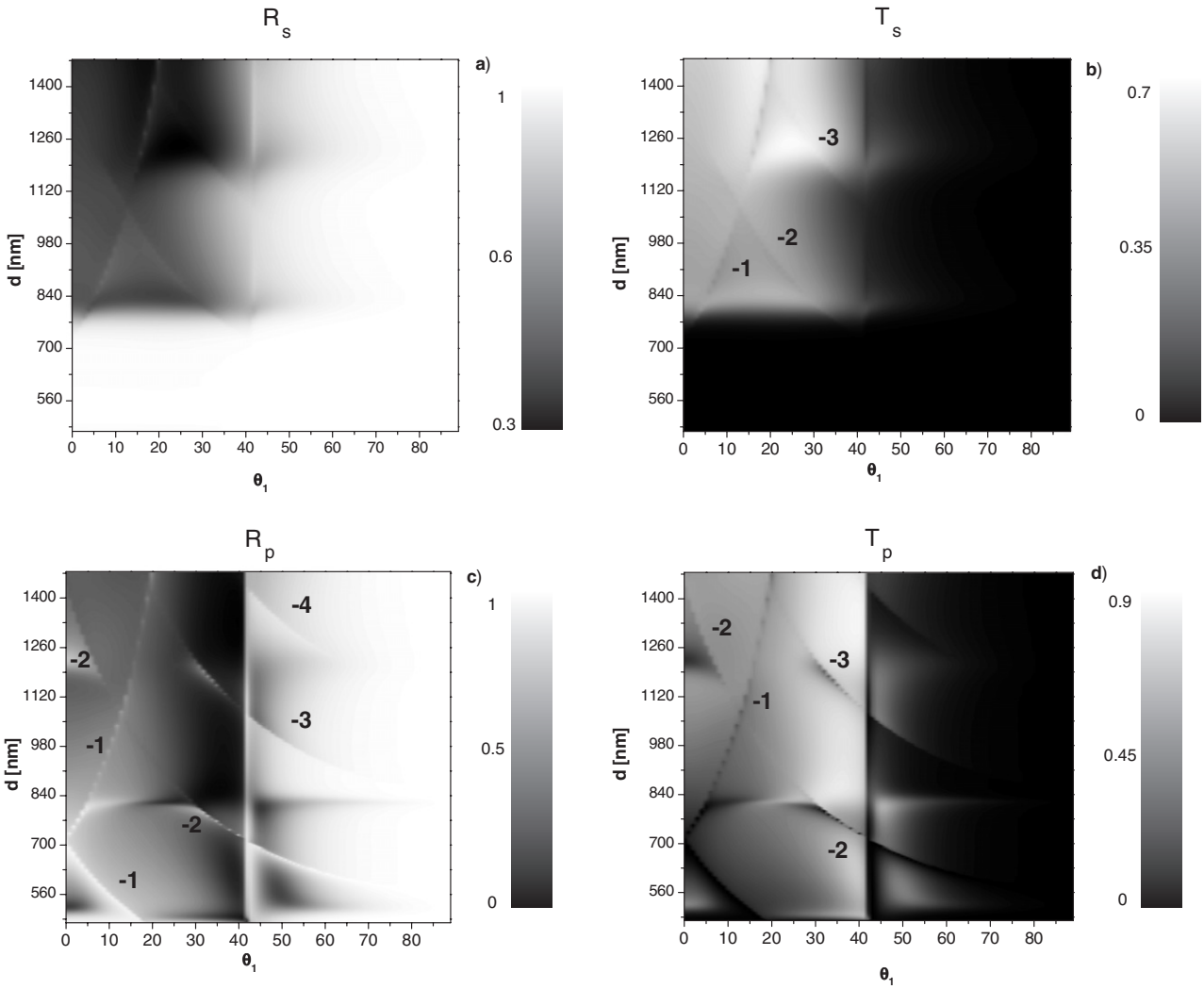

Figure 3. Maps of total reflected and transmitted intensity as a function of d and θ_1, for $\lambda_0 = 717$ nm, $h = 456.2$ nm, $e = 179.25$ nm, $\varepsilon_0 = 1$, $\varepsilon_1 = 2.25$, $\varepsilon_2 = -21.6 + i1.36$. (a) Reflected intensity and s polarization; (b) transmitted intensity and s polarization; (c) reflected intensity and p polarization; (d) transmitted intensity and p polarization.

polarizations, as it is expected for a decaying wave impinging on a periodic structure. The tunnel effect for s polarization is now much less significant: it occurs for a small interval of angles close to θ_c, and with a very low efficiency. For the p case, the response of the structure is similar to that observed for $e/\lambda_0 = 0.25$, with the difference that now the coupling of the incident evanescent wave with the SPP is produced in a narrower interval of angles. Then, for a given d, the transmission peak is more narrow, and less intense (it reaches up to 40% of the incident power, at most).

3.3. Rayleigh anomalies

A set of curves is easily identified in the maps of figures 3 and 4. These curves correspond to the Rayleigh anomalies i.e., to the combination of d, λ_0 and θ_1 which produce a grazing diffraction order, and these orders are indicated in figure 3. It is well known that when this condition is satisfied, the efficiency of the propagating diffraction orders exhibit sudden variations [14, 17, 45]. In figure 3(c) it is observed that these curves are light (in a dark background), not only for incident propagating waves ($\theta_1 < \theta_c$), but also for incident evanescent waves ($\theta_1 > \theta_c$). This denotes an increase in the total reflected intensity.

It is interesting to notice that when a Rayleigh anomaly crosses a region of high transmission (figure 3(d) for 473 nm $\leqslant d \leqslant$ 840 nm and $\theta_c < \theta_1 < 55°$), it redirects the power backwards to the incident medium, increasing the reflectivity of the structure in resonant form [14, 17, 45] (see figure 4 in [3]). In figure 3(d) this appears as a dark zone crossing the light region. This effect can be understood if we take into account that, at the Rayleigh condition, a grazing evanescent order in the dielectric interface is allowed. Its physical behaviour is similar to a surface wave, (a singularity is found in the reflection/transmission coefficients [17]), in which case the incident power is mainly reflected in resonant form. Then, for a fixed period d, a wide transmission peak (more than 10° wide) is obtained if $d < 616$ nm or if 717 nm $< d <$ 840 nm. However, for 616 nm $< d <$ 717 nm, the total transmitted intensity is crossed by the minimum produced by the Rayleigh

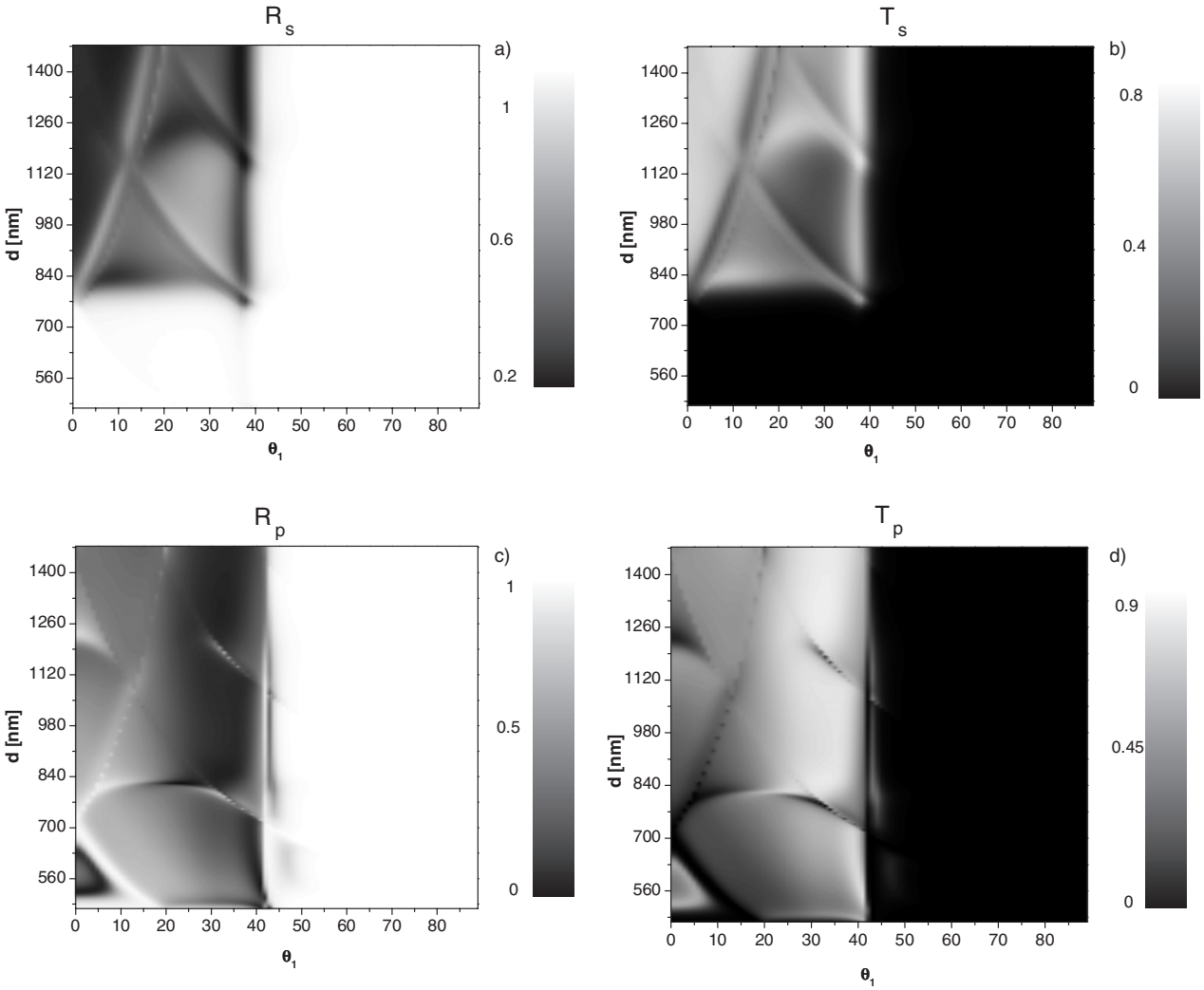

Figure 4. Same as figure 3 for $e = 537.75$ nm.

anomaly. This means that there are two transmission peaks within the interval $\theta_c < \theta_1 < 55°$.

Also in figure 4 the Rayleigh anomaly curves are very well defined in the upper left region of the s maps (figures 4(a) and (b)), and in the $\theta_1 < \theta_c$ region in the p maps.

4. Summary and discussion

We have studied different kinds of structural resonances that take place in a system formed by a periodic array of metallic cylinders and a planar dielectric interface. To solve the diffraction problem we adapted the modal method, which was found to be very suitable for the rectangular cross section of the wires. Since the structure is illuminated from the dielectric medium, propagating as well as evanescent incidences have been considered.

The results show the existence of both structural and SPP resonances. The first ones appear for propagating incidences, i.e., when the angle of incidence is smaller than the critical angle, and for large ratios λ_0/d. These structural resonances are due to constructive multiple reflection of the electromagnetic waves between the array and the planar dielectric interface. At the resonance condition, the electromagnetic field is confined in the gap formed between the array and the planar interface, and the whole system behaves like a planar waveguide. The number of minima in the reflectivity (resonant condition) increases with the distance between the array and the interface, and in this regime the array behaves like a thin film.

On the other hand, surface plasmons come into play when the period of the structure is increased. In this case, when the periodic wire structure is illuminated by an evanescent wave, surface plasmons and evanescent waves can be diffracted into reflected and transmitted propagating waves in the directions given by the diffraction orders allowed in the configuration.

In particular we showed that for a given set of geometrical parameters and when an efficient excitation of an eigenmode occurs, enhanced transmission can be achieved for the p mode. This enhancement is of about five orders of magnitude greater than the s transmission in the same situation. Notice that even without full optimization of the geometrical and constitutive parameters, an important resonant transmission is obtained, about 60% of the incident power. Thus it is possible to optimize

the device for a particular purpose. This enhanced transmission property could be interesting for applications such as filters, polarizers, electromagnetic switches or efficient multiplexed coupling devices.

Recently, the electrochemical synthesis of metal nanowires, together with electron beam lithography, allowed the production of metal nanowires with diameters of a few tens of nanometres and finite lengths in the micron regime [46]. The realization of samples in the nanometre scale opens up new applications for the results shown in this paper. For instance, they can be used to increase the light extraction efficiency in solid state light-emitting diodes (LEDs). In these devices, the relative refractive index between the external LED's face and air is bigger than unity (e.g., the refraction index for GaN is about 2.8) and, due to the critical angle, only a narrow light cone emerges from the LED. The light impinging with larger angles is reflected into the substrate and it is repeatedly reflected and reabsorbed by active layers or electrodes. With a suitable nanograting deposited on a glass substrate, with a thickness of about $\lambda_0/4$ and a refraction index smaller than that of the external LED cover (i.e. indium tin oxide doped glass, refraction index $\approx$1.7 [47]), it is possible to couple evanescent p waves to propagating transmitted modes by increasing the light extraction from the LED. As illustrated in figure 3(d), an efficient transmission for a wide range of incidence angles can be obtained with a suitable choice of geometrical parameters.

Acknowledgments

The authors gratefully acknowledge partial support from Consejo Nacional de Investigaciones Científicas y Técnicas (CONICET), Universidad de Buenos Aires (UBA), Universidad Nacional de la Provincia de Buenos Aires (UNICEN) and Agencia Nacional de Promoción Científica y Tecnológica (ANPCYT-BID 802/OC-AR03-14099). We thank Dr Ricardo Depine and Dr Héctor Ranea Sandoval for discussions. This work was also supported by a grant of Red Argentina de Optica y Fotofísica.

References

[1] Porto J, García-Vidal F J and Pendry J 1999 Transmission resonances on metallic grating with very narrow slits *Phys. Rev. Lett.* **83** 2845–8
[2] Astilean S, Lalanne Ph and Palamaru M 2000 Light transmission through metallic channels much smaller than the wavelength *Opt. Commun.* **175** 265–73
[3] Takakura Y 2001 Optical resonances in a narrow slit in a thick metallic screen *Phys. Rev. Lett.* **24** 5601–3
[4] García-Vidal F J, Martin-Moreno L, Lezec H and Ebbesen T 2003 Focusing light with a single subwavelength aperture flanked by surface corrugations *Appl. Phys. Lett.* **83** 4500–2
[5] Ebbesen T W, Lezec H J, Ghaemi H F, Thio T and Wolff P A 1998 Extraordinary optical transmission through sub-wavelength hole arrays *Nature* **391** 667–9
[6] Martin-Moreno L, García-Vidal F J, Lezec H J, Pellerin K M, Thio T, Pendry J B and Ebbesen T W 2001 Theory of extraodinary optical transmission through subwavelength hole arrays *Phys. Rev. Lett.* **86** 1114–7
[7] Krishnan A, Thio T, Kim T J, Lezec H J, Ebbesen T W, Wolff P A, Pendry J, Martin-Moreno L and García-Vidal F J 2001 Evanescently coupled resonance in surface plasmon enhanced transmission *Opt. Commun.* **200** 1–7
[8] Born M and Wolf E 1999 *Principles of Optics* 7th edn (Cambridge: Cambridge University Press)
[9] Stratton J A 1941 *Electromagnetic Theory* (New York: McGraw-Hill)
[10] Wood R W 1902 On a remarkable case of uneven distribution of light in a diffraction grating spectrum *Phil. Mag.* **4** 396
[11] Maradudin A A, Wallis R F and Dobrzynsky L 1980 Surface phonons and polaritons *Handbook of Surfaces and Interfaces* vol 3 (New York: Garland STPM Press)
[12] Girard Ch, Joacim Ch and Cautheir S 2000 The physics of the near-field *Rep. Prog. Phys.* **63** 893–938
[13] Raether H 1988 *Surface Polaritons on Smooth and Rough Surfaces and on Gratings* (Berlin: Springer)
[14] Lester M and Depine R 1996 Reflection of electromagnetic waves from index-matched surfaces *Opt. Commun.* **127** 189–92
[15] Pendry J B, Martin-Moreno L and García-Vidal F J 2004 Mimicking surface plasmons with structured surfaces *Science* **305** 847–8
[16] Lord Rayleigh 1907 *Proc. R. Soc.* A **79** 399
[17] Petit R (ed) 1980 *Electromagnetic Theory of Gratings* (Berlin: Springer)
[18] Thio T, Pellerin K M, Linke R A, Lezec H J and Ebbesen T W 2001 Enhanced light transmission through a single subwavelength aperture *Opt. Lett.* **26** 1972–4
[19] Muller R, Malyarchuk V and Lienau Ch 2003 Three-dimensional theory on light-induced near-field dynamics in a metal film with a periodic array of nanoholes *Phys. Rev.* B **68** 205415
[20] Degiron A and Ebbesen T W 2005 The role of localized surface plasmon modes in the enhanced transmission of periodic subwavelength apertures *J. Opt. A: Pure Appl. Opt.* **7** S90–6
[21] Skigin D C and Depine R A 2005 Transmission resonances on metallic compound gratings with subwavelength slits *Phys. Rev. Lett.* **95** 217402
[22] García-Vidal F J and Martin-Moreno L 2002 Transmission and focusing of light in one-dimensional periodically nanostructures metals *Phys. Rev.* B **66** 155412
[23] Depine R A and Ledesma S 2004 Direct visualization of surface-plasmon bandgaps in the diffuse background of metallic gratings *Opt. Lett.* **29** 2216–8
[24] Cites J, Sanghadasa M F M and Sung C C 1992 Analysis of photon scanning tunneling microscope images *J. Appl. Phys.* **71** 7–10
[25] Mulin D, Girard C, Colas des Francs G, Spajer M and Courjon D 2000 Near-field optical probing of two-dimensional photonic crystals: theory and experiment *J. Microsc.* **202** 110–6
[26] Kim D S, Hohng S C, Malyarchuk V, Yoon Y C, Ahn Y H, Yee K J, Park J W, Kim J, Park Q H and Lienau C 2003 Microscopic origin of surface-plasmon radiation in plasmonic band-gap nanostructures *Phys. Rev. Lett.* **91** 143901
[27] Fang N, Lee H, Sun C and Zhang X 2005 Sub-diffraction-limited optical imaging with a silver superlens *Science* **308** 534–7
[28] Tetz K A, Rokitski R, Nezhad M and Fainman Y 2005 Excitation and direct imaging of surface plasmon polariton modes in a two-dimensional grating *Appl. Phys. Lett.* **86** 111110
[29] Dintinger J, Klein S, Bustos F, Barnes W L and Ebbesen T W 2005 Strong coupling between surface plasmon–polaritons and organic molecules in subwavelength hole arrays *Phys. Rev.* B **71** 035424
[30] Byun K M, Kim S J and Kim D 2005 Desing study of highly sensitive nanowire-enhanced surface plasmon resonance biosensors using rigorous coupled wave analysis *Opt. Express* **13** 3737–42
[31] Dakss M L, Kuhn L, Heidrich P F and Scott B A 1970 Grating coupler for efficient excitation of optical guided waves in thin films *Appl. Phys. Lett.* **16** 523–5

[32] Brauer R and Bryngdahl O 1997 From evanescent waves to specified diffraction orders *Opt. Lett.* **22** 754–6
[33] Park S, Lee G, Song S H, Oh C H and Kim P S 2003 Resonant coupling of surface plasmons to radiation modes by use of dielectric gratings *Opt. Lett.* **28** 1870–2
[34] Sharon A, Glasberg S, Rosenblatt D and Friesem A A 1997 Metal-based resonant grating waveguide structures *J. Opt. Soc. Am.* A **14** 588–95
[35] Steele J M, Moran C E, Lee A, Aguirre C M and Halas N J 2003 Metallodielectric gratings with subwavelength slots: optical properties *Phys. Rev.* B **68** 205103
[36] Lochbihler H and Depine R 1993 Diffraction from highly conducting wire gratings *Appl. Opt.* **32** 3459–65
[37] Wang J J, Zhang W, Deng X, Deng J, Liu F, Sciortino P and Chen L 2005 High-performance nanowire-grid polarizers *Opt. Lett.* **30** 195–7
[38] Jackson J D 1975 *Classical Electrodynamics* 2nd edn (New York: Wiley)
[39] Coon D 1966 Counting photons in the optical barrier penetration experiment *Am. J. Phys.* **34** 240–3
[40] Coudonnet J, Inagaki T, Arakawa E and Ferrell T 1987 Angular and polarization dependence of surface-enhanced Raman scattering in attenued-total-reflection geometry *Phys. Rev.* B **36** 917–21
[41] Boltasseva A, Nikolajsen T, Leosson K, Kjer K, Larsen M and Bozhevolnyi S 2005 Integrated optical components utilizing long-range surface plasmon polaritons *J. Lightwave Technol.* **23** 413–22
[42] Podolskiy V, Sarychev A, Narimanov E and Shalaev V 2005 Resonant light interaction with plasmonic nanowire systems *J. Opt. A: Pure Appl. Opt.* **7** S32–7
[43] Gilberd P 1982 The anomalous skin effect and the optical properties of metals *J. Phys. F. Met. Phys.* **12** 1845–60
[44] Kottmann J P, Martin O J F, Smith D R and Schultz S 2001 Plasmon resonances of silver nanowires with a nonregular cross section *Phys. Rev.* B **64** 5402
[45] Lester M and Depine R 1996 Scattering of electromagnetic waves at the corrugated interface between index-matched media *Opt. Commun.* **132** 135–43
[46] Schider G, Krenn J R, Gotschy W, Lamprecht B, Ditlbacher H, Leitner A and Aussenegg F R 2001 Optical properties of Ag and Au nanowire gratings *J. Appl. Phys.* **90** 3825–30
[47] Chiou B-S and Tsai J-H 1999 Antireflective coating for ITO films deposited on glass substrate *J. Mater. Sci. Mater. Electron.* **10** 491–5
Djurišìc A, Guo W L, Li E H, Lam L S M, Chan W K, Adachi S, Liu Z T and Kwok H S 2001 Optical properties of optical polycarbonate layers *Opt. Commun.* **197** 355–61